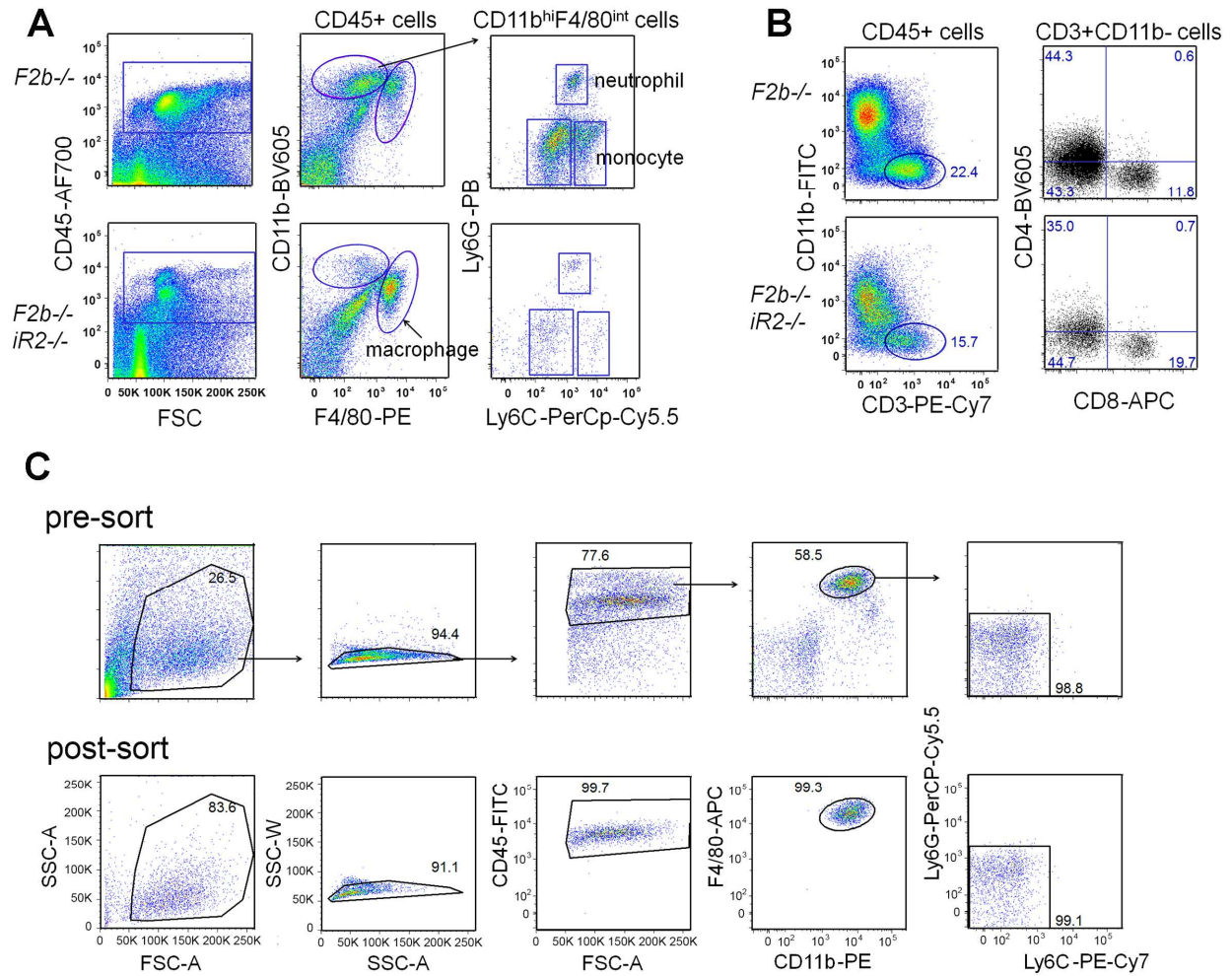


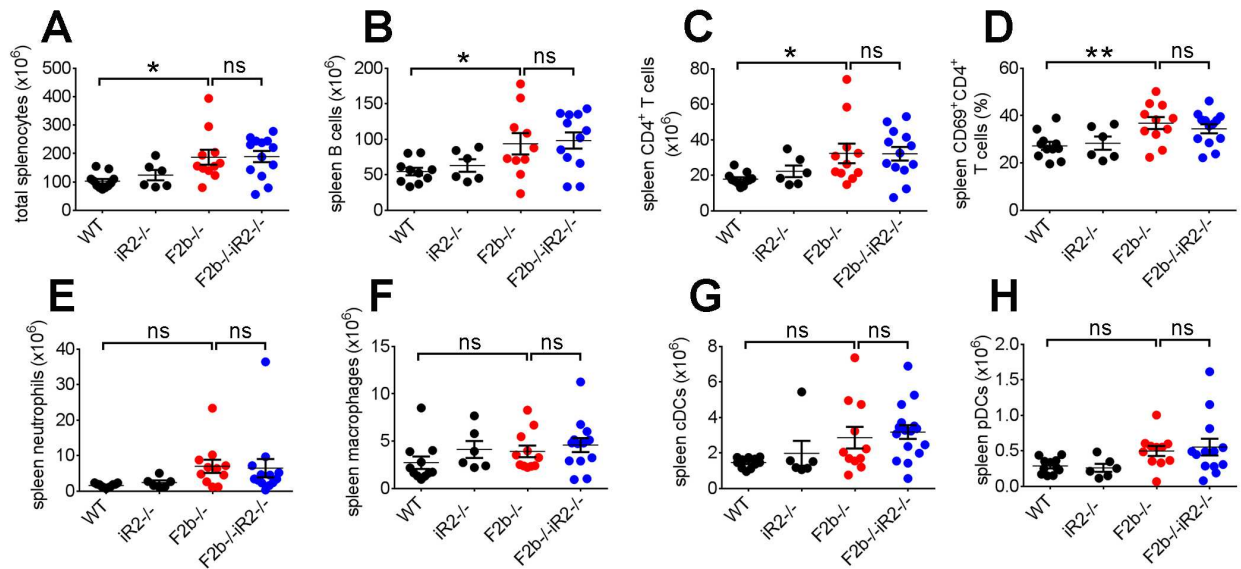
SUPPLEMENTAL FIGURES

Sup. Figure 1



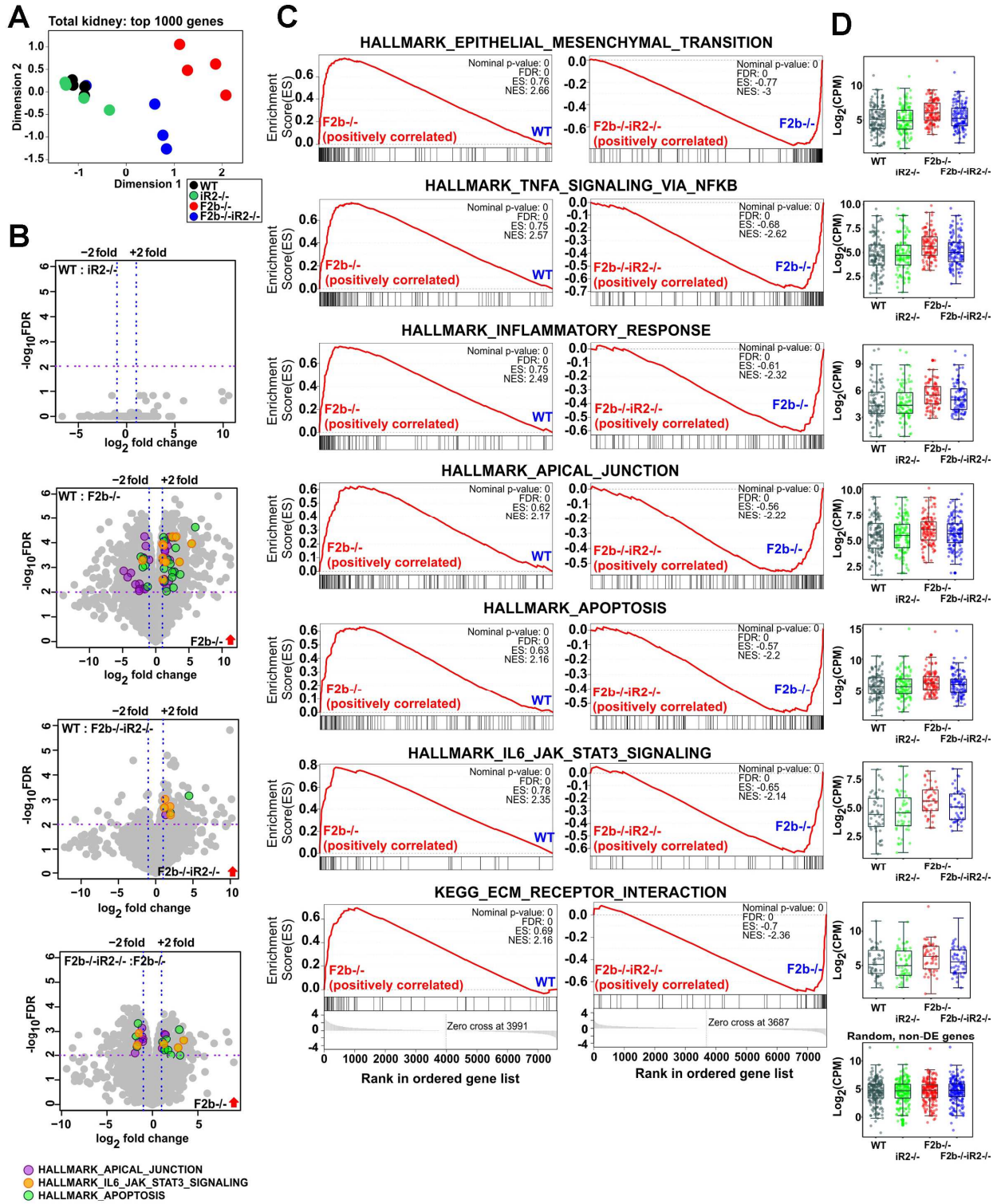
Supplemental figure 1. Flow cytometry gating and sorting strategies. (A and B) Gating strategy for flow cytometry analysis of inflammatory cell infiltrates in the kidneys. (A) CD45⁺ leukocytes, CD45⁺F4/80^{hi}CD11b⁺ macrophages, CD45⁺F4/80^{int}CD11b^{hi}Ly6C⁺Ly6G⁺ neutrophils, CD45⁺F4/80^{int}CD11b^{hi}Ly6C^{hi}Ly6G⁻ Ly6C^{hi} monocytes. (B) T cell subsets (CD45⁺CD11b⁻CD3⁺ total T cells, CD45⁺CD11b⁻CD3⁺ CD4⁺CD8⁻ T cells, CD45⁺CD11b⁻CD3⁺CD4⁻CD8⁺ T cells, and CD45⁺CD11b⁻CD3⁺CD4⁻CD8⁻ double negative T cells). (C) Sorting macrophages from kidneys for RNA-seq. Macrophages were sorted as CD45⁺F4/80^{hi}CD11b⁺Ly6G⁻Ly6C⁻ population in perfused kidneys for RNA-seq.

Sup. Figure 2



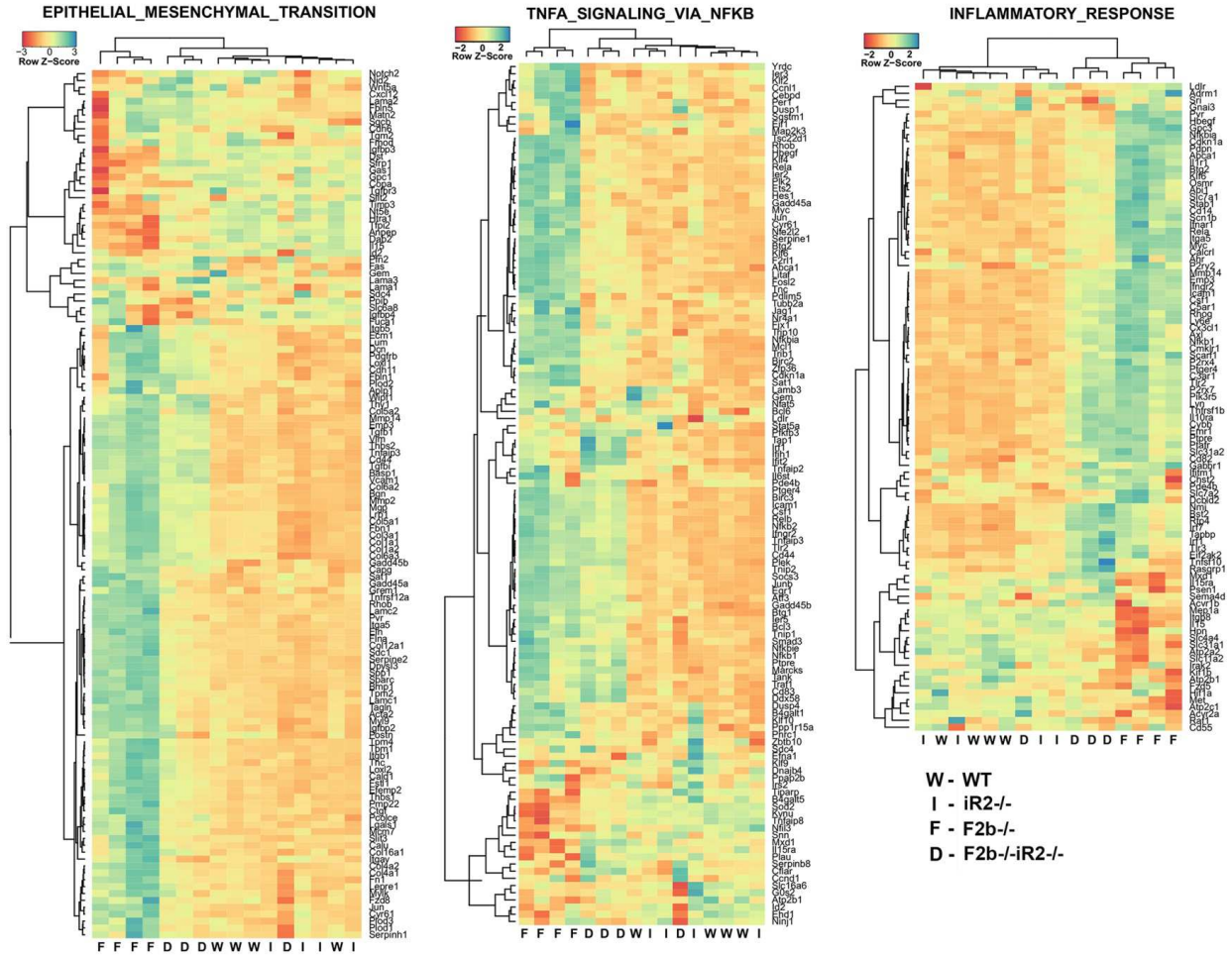
Supplemental Figure 2. Expansion of immune cells in the spleen of *Fcgr2b*^{-/-} mice was not affected by *iRhom2* deficiency. Spleen cells from 7-9 month old mice were assessed by flow cytometry. (A) Numbers of total splenocytes. (B) Numbers of CD11b⁻CD3⁺B220⁺CD4⁻ B cells. (C) CD11b⁻CD3⁺B220⁻CD4⁺ T cells. (D) Percentage of CD69⁺ activated CD4⁺ T cells. (E) Numbers of CD11b^{hi}Ly6G⁺ neutrophils. (F) F4/80^{hi}CD11b⁺ macrophages. (G) CD11c^{hi}MHCclassII⁺PDCA⁻ conventional dendritic cells (cDCs). (H) CD11c^{lo}PDCA⁺ plasmacytoid dendritic cells (pDCs). A-H, 11 *WT*, 6 *Rhbd2*^{-/-}, 11 *Fcgr2b*^{-/-}, and 13 *Fcgr2b*^{-/-}*Rhbd2*^{-/-} mice. All are mean ± s.e.m, One-way ANOVA with Dunnett's multiple comparisons test. * *P*<0.05, ** *P*<0.01, ns, not significant.

Sup. Figure 3



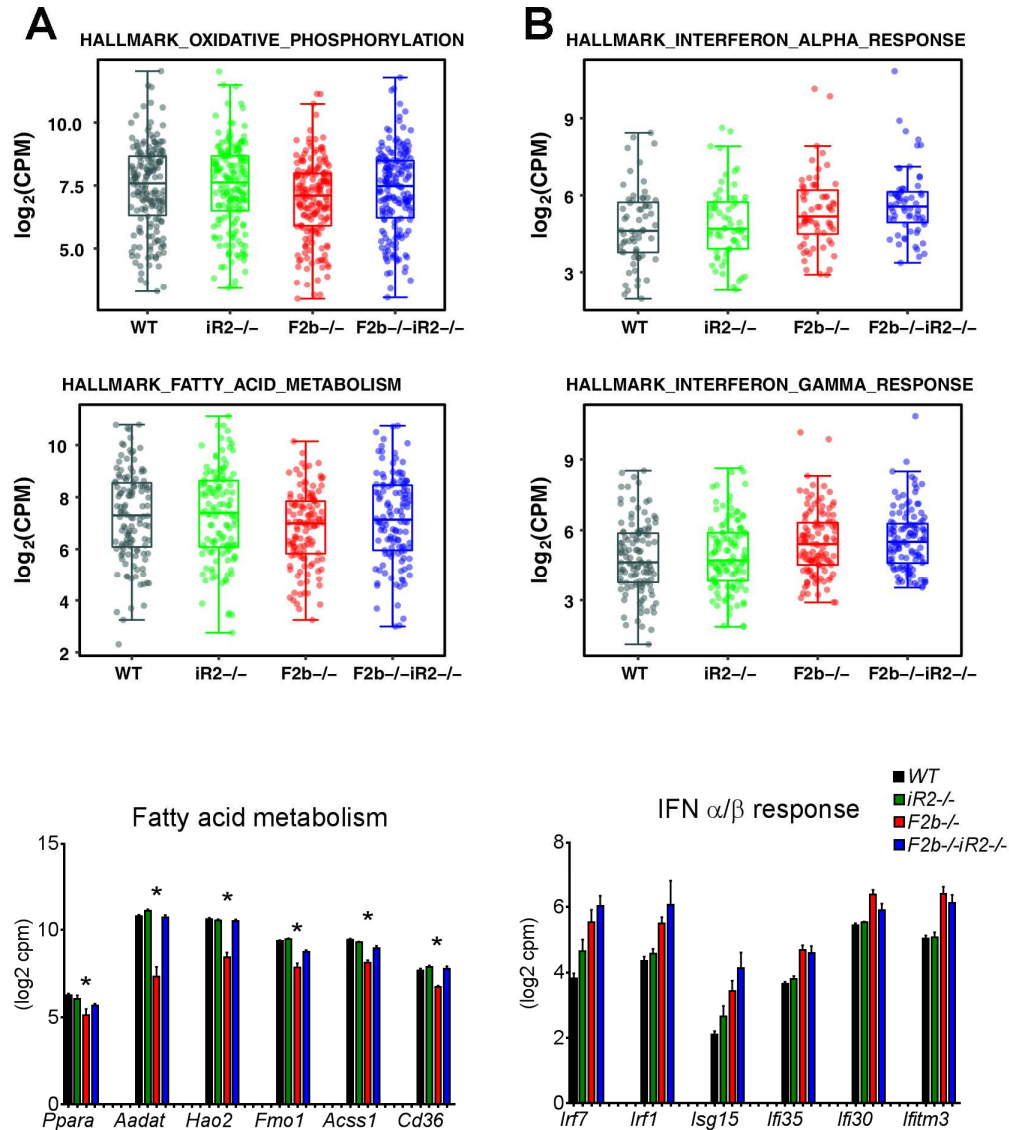
Supplemental figure 3. RNA-seq profiling of mouse kidneys. (A) Multidimensional scaling plot for the top 1000 genes with the largest expression variance identified by RNA-seq. (B-D) GSEA of RNA-seq data. (B) Differentially expressed genes that belonged to the hallmark gene sets in *Fcrg2b*^{-/-} vs. WT mice were highlighted in the volcano plots. (C) GSEA profiles for the top hallmark gene sets are shown for *Fcrg2b*^{-/-} vs. WT (left panels) and *Fcrg2b*^{-/-} vs. *Fcrg2b*^{-/-} *Rhbd2*^{-/-} kidneys (right panels). FDR, False discovery rate. ES, Enrichment score. NES, Normalized enrichment score. (D) Expression of genes from hallmark gene sets is illustrated for all 4 groups of mice. A set of random non-differentially expressed genes (*n*=200) were shown as control on the bottom. (*n*=4 mice per group)

Sup. Figure 4



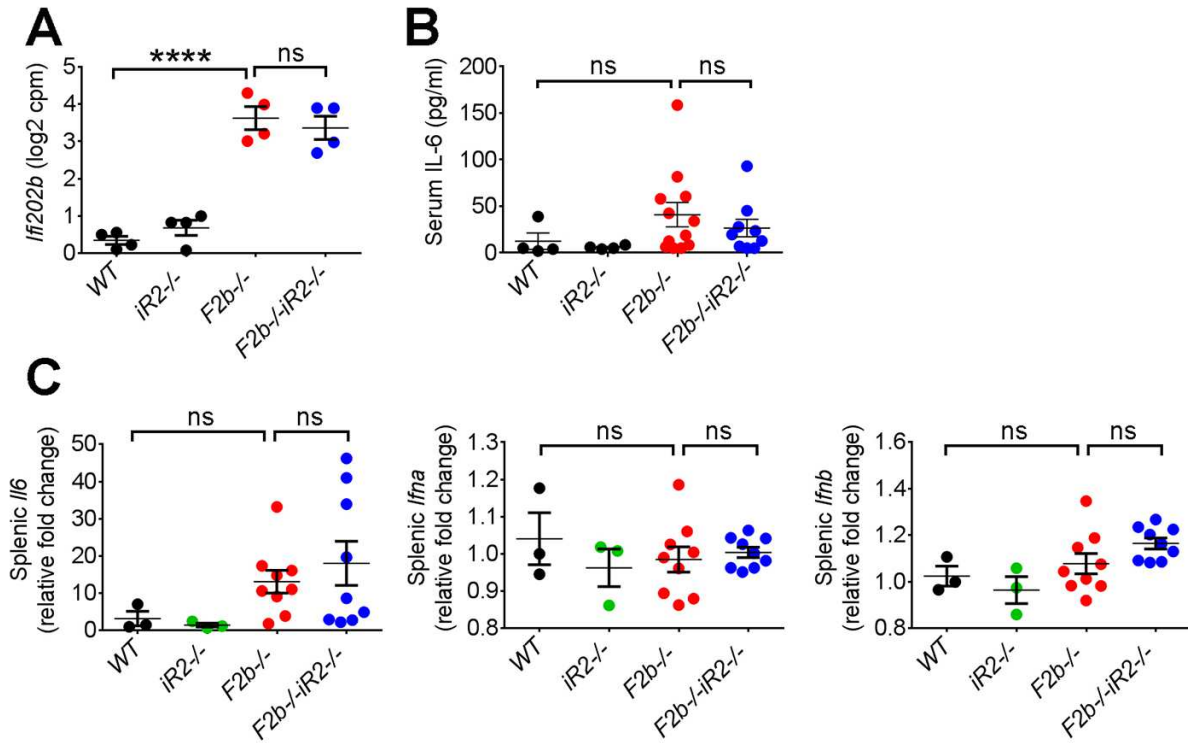
Supplemental figure 4. Hierarchical clustering of genes from the EMT, TNF signaling and inflammatory response gene sets in mouse kidneys. GSEA of RNA-seq data from lupus kidneys identified the EMT, TNF signaling and inflammatory response as the top 3 hallmark gene sets differentially expressed between *Fcrg2b*^{-/-} vs. WT mice. Unsupervised hierarchical clustering indicates substantial upregulation of genes from these gene sets in *Fcrg2b*^{-/-} compared to other genotypes ($n=4$ mice per group).

Sup. Figure 5



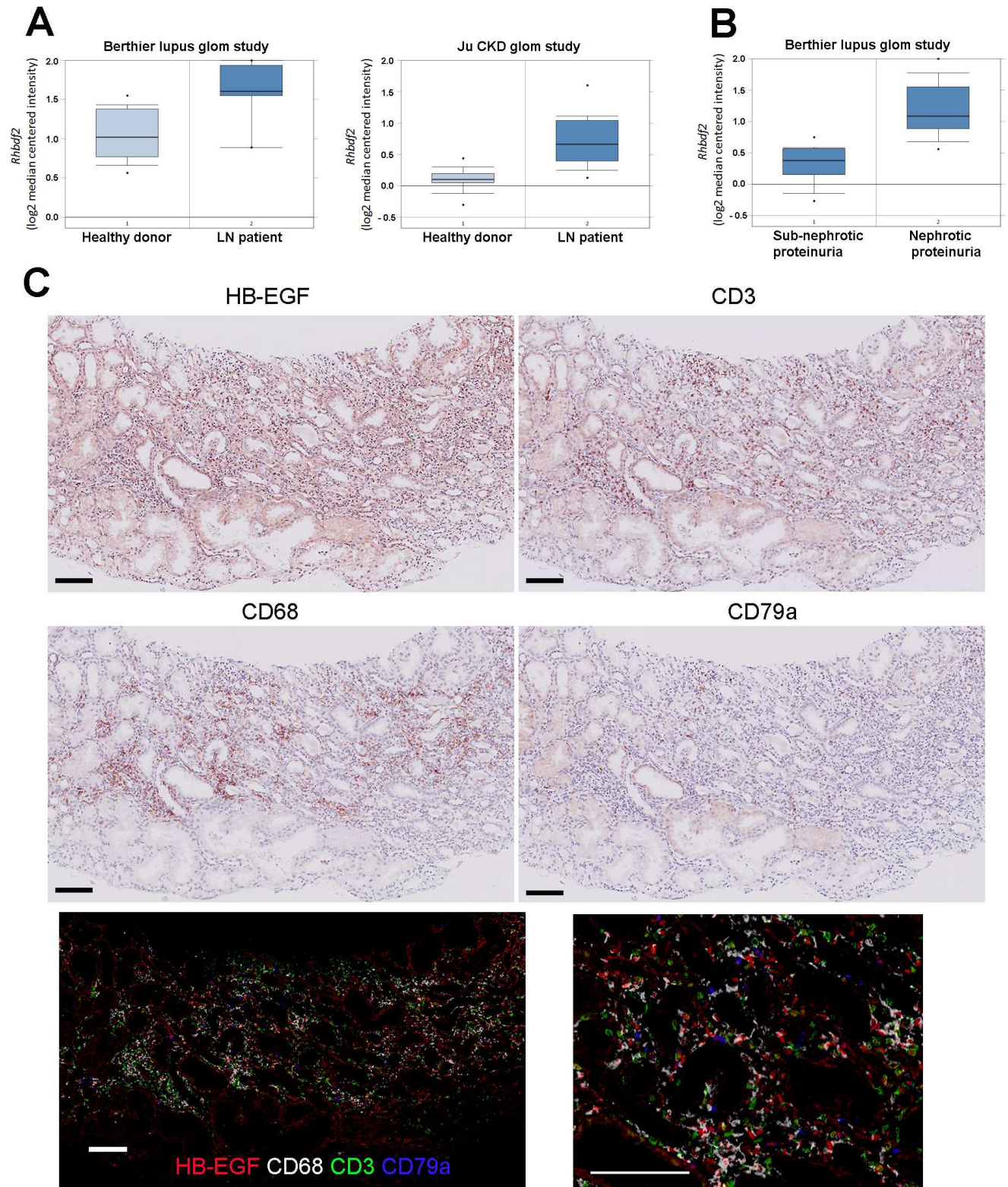
Supplemental figure 5. Fatty acid metabolism and IFN responses in the kidneys of *Fcrg2b*^{-/-} mice. GSEA was performed on RNA-seq results from total kidneys. Expression of gene sets encoding oxidative phosphorylation, fatty acid metabolism (A) and IFN α , IFN γ responses (B) was illustrated. Representative genes shown: *Ppara*, peroxisome proliferative activated receptor, alpha; *Aadat*, amino adipate aminotransferase; *Hao2*, hydroxyacid oxidase 2 (long chain); *Fmo1*, flavin containing monooxygenase 1; *Acsc1*, acyl-CoA synthetase short-chain family member 1; *Cd36*, thrombospondin receptor; *Irf7*, interferon regulatory factor 7; *Irf1*, interferon regulatory factor 1; *Isg15*, ISG15 ubiquitin-like modifier; *Ifi35*, interferon-induced protein 35; *Ifi30*, interferon-induced protein 30; *Ifitm3*, interferon induced transmembrane protein 3. $n=4$ mice per group. * $P<0.05$

Sup. Figure 6



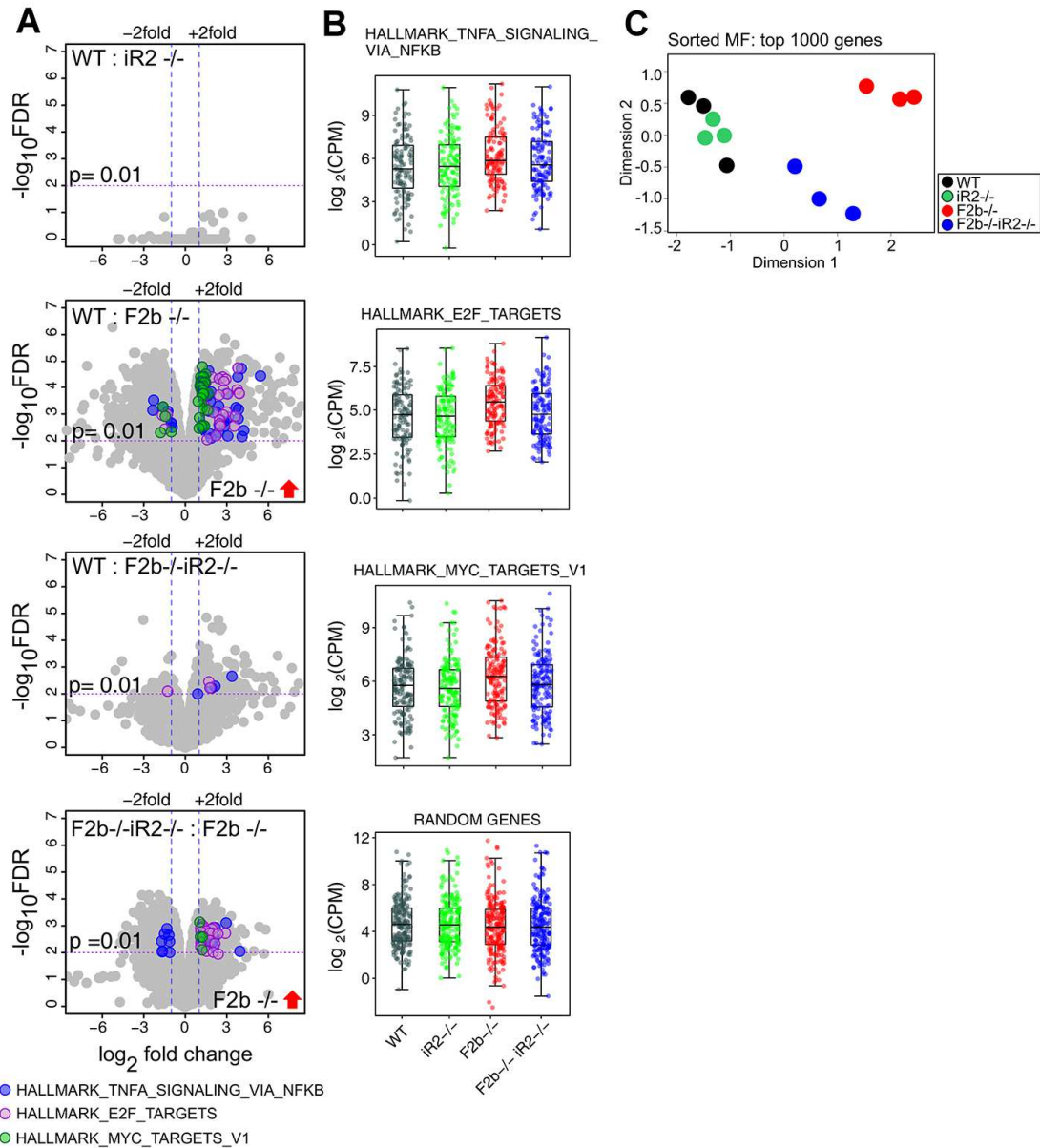
Supplemental Figure 6. Type I IFN induced genes and serum IL-6 are not altered by *iRhom2* deficiency in *Fcgr2b*^{-/-} mice. (A) Expression of *Ifi202b* in the kidneys on RNA-seq. *n*=4 mice per group, mean ± s.e.m. (B) IL-6 was measured by ELISA in the serum of WT (*n*=4), *Rhbd2*^{-/-} (*n*=4), *Fcgr2b*^{-/-} (*n*=12) and *Fcgr2b*^{-/-}*Rhbd2*^{-/-} mice (*n*=10) at the age of 7-9 months upon euthanasia. (C) Expression of *Il6*, *Ifna*, and *Ifnb* mRNA in the spleen measured by qPCR. 3 WT, 3 *Rhbd2*^{-/-}, 9 *Fcgr2b*^{-/-} and 9 *Fcgr2b*^{-/-}*Rhbd2*^{-/-} mice. Mean ± s.e.m. (B and C) One-way ANOVA with Dunnett's multiple comparisons test. **** *P*<0.0001, ns, not significant.

Sup. Figure 7



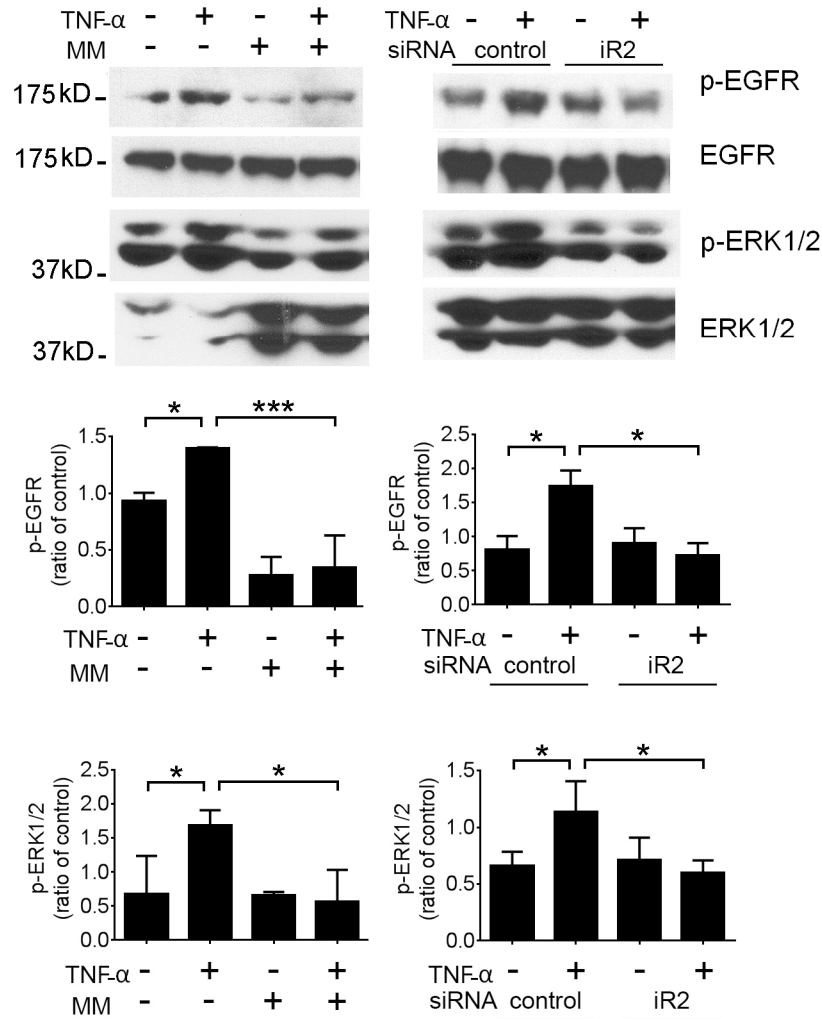
Supplemental figure 7. *Rhbdf2* and HB-EGF are over-expressed in the kidneys of LN patients. (A and B) Expression of *Rhbdf2* in kidneys of LN patients measured by cDNA microarray. (A) Healthy donors vs. LN patients. Berthier lupus glom study, 14 healthy donor and 32 LN patients, mean \pm s.d., fold change=1.813, $P=6.00E-10$ (35) (GSE32591); Ju CKD glom study, 21 healthy donor and 32 LN patients, mean \pm s.d., fold change=1.532, $P=2.99E-10$ (34). (B) Patients with sub-nephrotic proteinuria vs. patients with nephrotic proteinuria. Berthier lupus glom study, 18 patients with sub-nephrotic proteinuria and 9 patients with nephrotic proteinuria, fold change=1.518, $P=2.69E-10$ (35) (GSE32591). (C) Sequential staining of HB-EGF (red signal) and leukocytes in the kidney interstitium of LN patients. CD68 (white signal) for macrophages, CD3 (green signal) for T cells and CD79a (blues signal) for B cells. Scale bar, 100 μ m. Representative image from 24 LN patients (18 class IV and 6 class V). This data is also shown in Figure 10B.

Sup. Figure 8



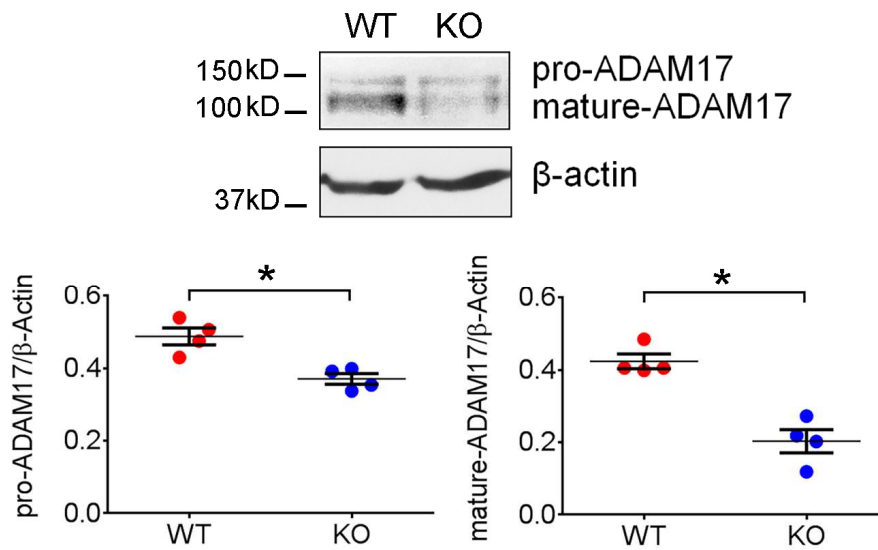
Supplemental figure 8. RNA-seq analysis of kidney macrophages from *Fcgr2b*^{-/-} mice. (A) Volcano plots of genes differentially expressed between each group ($P=0.01$, $FC=2$). Differentially-expressed genes that belong to the enriched hallmark gene sets identified by GSEA are shown in indicated colors. **(B)** Expression of genes from TNF signaling, E2F targets and Myc targets gene sets. A set of random non-differentially expressed genes ($n=200$) is shown as control. **(C)** Multidimensional scaling plot for the top 1000 genes with the largest expression variance identified by RNA-seq.

Sup. Figure 9



Supplemental figure 9. TNF- α transactivates EGFR via the iRhom2/ADAM17 pathway in kidney tubular epithelial cells. C1 cells pretreated with MM or transfected with siRNA were stimulated with mouse recombinant TNF- α . Expression of p-EGFR, EGFR, p-ERK1/2 and ERK1/2 was assessed in cell lysates. The p-EGFR/EGFR and p-ERK1/2/ERK bands in the siRNA experiments shown here are replicate samples run on parallel gels. P-EGFR and p-ERK1/2 expression was calculated as ratios against total EGFR or ERK1/2 respectively. n=3 independent experiments, mean \pm s.e.m. One-way ANOVA with Dunnett's multiple comparisons test. * $P < 0.05$, *** $P < 0.001$.

Sup. Figure 10



Supplemental figure 10. Decreased ADAM17 expression in the nephrons of *iRhom2* deficient mice. Nephrons (glomeruli and tubules) isolated from *Rhbd2*^{-/-} and WT mice were examined for ADAM17 expression (pro- and mature forms). n=4 mice per group, β -actin ratio as loading control, mean \pm s.e.m. two-tailed Mann-Whitney test. * $P < 0.05$.

Supplemental Table 1. Demographics of patients with kidney biopsies

Diagnosis	Kidney biopsies (n)	Age (Years, Mean \pm SD)	Female (n)	Male (n)
LN class IV with crescents	9	39 \pm 16	7	2
LN class IV without crescents	9	35 \pm 17	5	4
LN class V	6	44 \pm 15	4	2
ANCA associated vasculitis	10	56 \pm 18	4	6